AD-A116 264 ARIZONA UNIV TUCSON ENGINEERING EXPERIMENT STATION F/G 20/4
UNSTEADY TRANSONIC FLOWS: TIME-LINEARIZED CALCULATIONS,(U)
OCT 80 A R SEEBASS, K FUNG N00014-76-C-0182
UNCLASSIFIED TFD-80-03 NL

END
DATE FILMED
8-82
DTIC

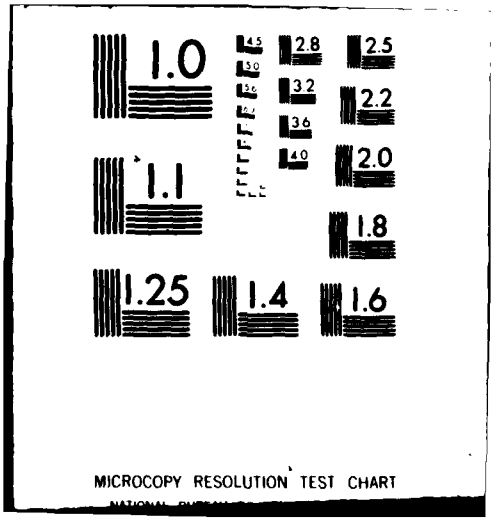
1.0
1.1
1.25
1.4
1.6
1.8
2.0
2.2
2.5
2.8
3.2
3.6
4.0
MICROCOPY RESOLUTION TEST CHART

TRANSONIC FLUID DYNAMICS

Report TFD 80-03

A. Richard Seebass and K.-Y. Fung

UNSTEADY TRANSONIC FLOWS: TIME-LINEARIZED CALCULATIONS

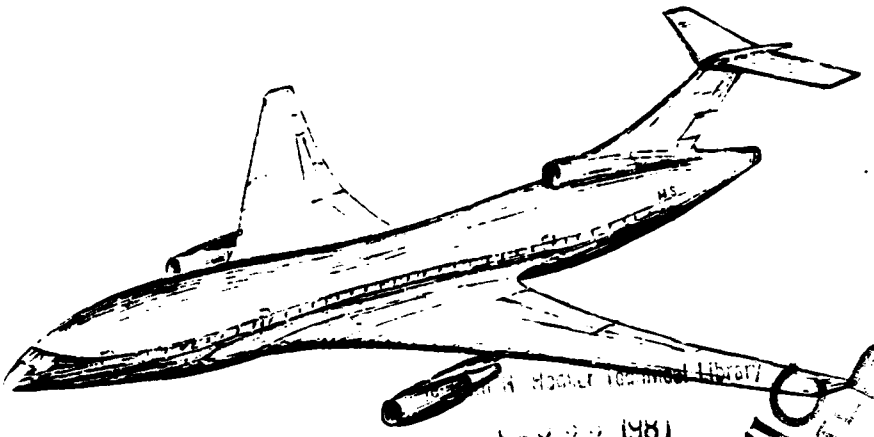

October 1980

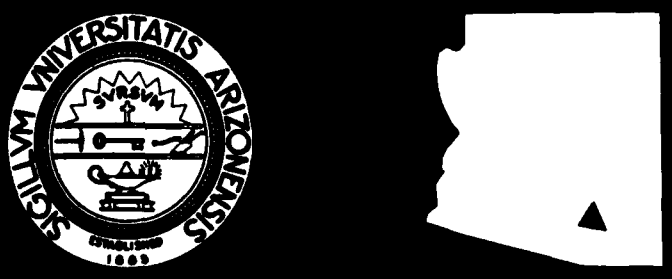

ENGINEERING EXPERIMENT STATION
COLLEGE OF ENGINEERING
THE UNIVERSITY OF ARIZONA
TUCSON, ARIZONA 85721

SECURITY CLASSIFICATION OF THIS PAGE *(When Data Entered)*

REPORT DOCUMENTATION PAGE

READ INSTRUCTIONS BEFORE COMPLETING FORM

1. REPORT NUMBER	2. GOVT ACCESSION NO. AD-A116 269 / 3. RECIPIENT'S CATALOG NUMBER
4. TITLE *(and Subtitle)* UNSTEADY TRANSONIC FLOWS: TIME-LINEARIZED CALCULATION	5. TYPE OF REPORT & PERIOD COVERED
	6. PERFORMING ORG. REPORT NUMBER TFD 80-03
7. AUTHOR(s) A. Richard Seebass and K.-Y. Fung	8. CONTRACT OR GRANT NUMBER(s) N00014-76-C-0182
9. PERFORMING ORGANIZATION NAME AND ADDRESS University of Arizona Aerospace and Mechanical Engineering Tucson, Arizona 85720	10. PROGRAM ELEMENT, PROJECT, TASK AREA & WORK UNIT NUMBERS
11. CONTROLLING OFFICE NAME AND ADDRESS Office of Naval Research (code 438) Arlington, Virginia 22217	12. REPORT DATE October 1980
	13. NUMBER OF PAGES 8
14. MONITORING AGENCY NAME & ADDRESS *(if different from Controlling Office)* Office of Naval Research Resident Representative Room 223 Bandeler Hall West University of New Mexico Albuquerque, NM 8713	15. SECURITY CLASS. *(of this report)* Unclassified
	15a. DECLASSIFICATION/DOWNGRADING SCHEDULE

16. DISTRIBUTION STATEMENT *(of this Report)*

Approved for Public Release: distribution unlimited.

17. DISTRIBUTION STATEMENT *(of the abstract entered in Block 20, if different from Report)*

18. SUPPLEMENTARY NOTES

19. KEY WORDS *(Continue on reverse side if necessary and identify by block number)*

Transonic Flow
Unsteady Flow

20. ABSTRACT *(Continue on reverse side if necessary and identify by block number)*

An accurate and efficient method of computing unsteady transonic flow is described. The flow is linearized about an experimentally measured or numerically calculated steady stae, as represented by a given pressure distribution. For a given mode of motion, the amplitudes and phase lags of the lift and moment coefficients at a given reduced frequency are found by superposition from an indicial response. The computational effort is reduced by treating shock waves as discontinuities, and by

DD FORM 1 JAN 73 1473 EDITION OF 1 NOV 65 IS OBSOLETE
S/N 0102-014-6601

SECURITY CLASSIFICATION OF THIS PAGE *(When Data Entered)*

applying the correct linear far-field behavior. A novel method of modeling the indicial response provides an analytical formulas for the dependence of the amplitude and phase lag on the reduced frequency.

TRANSONIC FLUID DYNAMICS

Report TFD 80-03

A. Richard Seebass and K.-Y. Fung

UNSTEADY TRANSONIC FLOWS: TIME-LINEARIZED CALCULATIONS

October 1980

UNSTEADY TRANSONIC FLOWS: TIME-LINEARIZED CALCULATIONS

A. Richard Seebass and K.-Y. Fung
Aerospace and Mechanical Engineering, University of Arizona, Tucson, Arizona

An accurate and efficient method of computing unsteady transonic flow is described. The flow is linearized about an experimentally measured or numerically calculated steady state, as represented by a given pressure distribution. For a given mode of motion, the amplitudes and phase lags of the lift and moment coefficients at a given reduced frequency are found by superposition from an indicial response. The computational effort is reduced by treating shock waves as discontinuities, and by applying the correct linear far-field behavior. A novel method of modeling the indicial response provides an analytical formulas for the dependence of the amplitude and phase lag on the reduced frequency.

INTRODUCTION

A combination of technical advances should improve the fuel efficiency of transport aircraft by fifty percent in the next decade. Analogous improvements in the transonic performance of military aircraft should also be realized. These large gains will come from a combination of improvements in engine, structural, and aerodynamic efficiency. More than half will come from improvements in the aerodynamic efficiency, including active control, and the use of composite materials in the primary structure. Part of the improvement in aerodynamic efficiency will result from flight at supercritical Mach numbers with subcritical levels of lift to drag ratio and high lift coefficients at near sonic flight conditions.

This improved transonic performance mandates an accurate prediction of aeroelastic behavior at transonic Mach numbers. Of special concern are flutter boundaries. In 1976 Farmer and Hanson (1) reported that the flutter boundaries of two dynamically identical wings were markedly different at transonic Mach numbers due to very minor differences in wing profile thickness. The results of their measurements are shown in Figure 1, indicating the reduced flutter boundary for the wing with a "supercritical" profile.

Today we understand well the qualitative behavior of inviscid steady and unsteady transonic flows, and we have rudimentary understanding of viscous effects. For flight regimes that involve unseparated flows the main ingredient in the calculation of flutter boundaries is an accurate determination of the steady pressure field. This may be determined either by experiment or by calculation. But once it is known, the response of the wing to pitching, plunging or aileron motion may be found by numerical means. The most essential ingredient in predicting this response is an accurate prediction of the motion of any shock waves present in the flow (see, e.g., (2)). Numerical algorithms that capture shock waves must use relatively fine grid spacing near the shock wave if they are to predict its motion due to the small changes of interest in flutter studies. But this shock motion may be predicted accurately by a time-linearized algorithm using a relatively coarse grid if the calculations are done correctly. This has not generally been the case, with other investigators ignoring this essential effect (3,4,5).

We report here on our two-dimensional, time-linearized computations, which not only properly account for shock wave motion, but are able to resolve them even though the grid used to calculate the flow is relatively coarse. In order to avoid the reflection of the unsteady disturbances from the grid system, only a moderate amount of grid stretching is employed away from the airfoil. To avoid unnecessarily large computational domains, the linearized far-field for an unsteady vortex with a circulation determined by the airfoil's lift is used to evaluate the potential there (6). The airfoil's response to a given mode of motion is determined by superposition from that for an indicial motion. In many cases this indicial response can be modeled in a simple way, providing an analytic result for the dependence of the lift and moment coefficient's amplitudes and phase lags on reduced frequency. A novel feature of this modeling is that of a sequence of harmonic oscillators, each of which improves the previous simulation of the indicial response. This provides an analytical formula for the dependence of the amplitudes and phase lags on the reduced frequency (7).

The computational efficiency of the time-linearized calculation of the amplitudes and phase lags for a range of reduced frequencies is compared with nonlinear and frequency domain computations. The time-linearized calculation of an indicial response can result in a factor of ten or more reduction in computational effort; this is especially significant in three dimensions. The modeling of the indicial response by a sequence of two harmonic oscillators can also reduce computational effort.

GOVERNING EQUATIONS

As noted above, time-linearization about a known steady state is an effective mechanism for determining the unsteady response to a given mode of motion. For flows that are unseparated, and not at incipient separation, an inviscid treatment of the unsteady flow should be adequate for flutter studies. It is important, however, that the nonlinear and viscous aspects of the underlying steady state be determined accurately. This may either be done by experiment, or by a reliable computational algorithm such as Grumfoil (8). In any case, we assume that an accurate steady state pressure distribution has been used to provide the input for the inverse calculation of the airfoil shape that will provide this pressure distribution when the steady state flow is

computed using the small perturbation approximation.

As Lin et al. (9) observed more than thirty years ago, within the context of the small perturbation approximation the basic equation governing the unsteady motions is linear unless the reduced frequency, k, is $O(\delta_o)$. Here δ_o is the measure of the perturbation potential and $k = \omega c/U$, where ω is the frequency, c the chord and U the freestream speed. Thus, if we write the velocity potential, ϕ, as

$$\phi = Uc\{x + \delta_o \varphi\}$$

where φ is the perturbation potential and δ_o is some measure of the disturbance, the governing equation is

$$-(2k/\delta_o)M_\infty^2\varphi_{xt} + \{(1 - M_\infty^2)/\delta_o - (\gamma + 1)M_\infty^2\varphi_x\}\varphi_{xx} \quad (1)$$

$$+ \varphi_{yy} = 0,$$

where terms $O(k^2\varphi_{tt}/\delta_o)$ and $O(k\varphi_t\varphi_{xx})$ have been neglected because $k = O(\delta_o)$. (Here the time has been nondimensionalized by the circular frequency and the spatial coordinates by the airfoil chord, and the y coordinate is scaled by $\delta_o^{1/2}$.) The second is of little consequence. Neglecting the first is equivalent to disregarding one of the characteristics and assuming disturbances propagate downstream at infinite speed, and has important computational advantages. The boundary condition at the body is

$$\delta_o^{3/2}\varphi_y(x,o,t) = \delta Y'(x) + \overline{\delta Y}_x(x,t) + k\overline{\delta Y}_t(x,t) \quad (2)$$

where the body is given by

$$y = \delta Y(x) + \overline{\delta Y}(x,t).$$

Across the airfoil wake the jump in the pressure coefficient must vanish. Thus,

$$[\![\, \tfrac{1}{2} C_p(x,o,t)]\!] = -[\![\varphi_x(x,o,t) + k\varphi_t(x,o,t)]\!] = 0,$$

where $[\![(\cdots)]\!]$ indicates the jump across the wake. This implies that in the wake

$$\Delta\phi(x,o,t) = \Gamma(x - kt)/Uc\delta_o. \quad (3)$$

In both these boundary conditions we have retained terms of O(k), which is not consistent with the approximation made in Eq. (1). But as Refs. (10) and (11) demonstrate, this gives good agreement with the results of linear theory for values of k up to, and even above, 1.0. This term is, of course, also retained in the evaluation of the pressure coefficients. As noted in Ref. (2), the appropriate measure of δ_o is $\max(\delta^{3/2}, \bar{\delta}^{3/2}, (k\delta)^{3/2})$ and normally $\delta^{3/2}$. Far from the airfoil (see (6)),

$$\varphi(x,y;t') = \frac{1}{2\pi}\int_o^{t'} f(x,y;t' - t_o')\frac{d\Gamma(t_o')}{dt_o'}\,dt_o' \quad (4)$$

where

$$f(x,y;t') = H(t' + x - \sqrt{(x^2 + y'^2)})\times$$
$$\tan^{-1}\frac{\sqrt{(t'^2 + 2xt' - y'^2)} + t'}{y'}$$

$$- \tan^{-1}\frac{\sqrt{(t'^2 + 2xt' - y'^2)} - t'}{y'}\},$$

and

$$t' = t(1 - M_\infty^2)/kM_\infty^2\,,\quad y' = y\sqrt{[(1 - M_\infty^2)/\delta_o]}.$$

Here H is the Heaviside unit step function.

In addition to Eq. (1) and the boundary conditions (2)-(4), a shock jump condition needs to be imposed if the shock wave is to be treated as a discontinuity rather than "captured" by the numerical calculations. Because the former is the intent here, we need to note that

$$-(2kM_\infty^2/\delta_o)[\![\varphi_x]\!]^2(dx/dt)_s$$
$$-[(1 - M_\infty^2)/\delta_o - (\gamma + 1)M_\infty^2\overline{\varphi_x}]\,[\![\varphi_x]\!]^2 + [\![\varphi_y]\!]^2 = 0, \quad (5a)$$

on

$$(dy/dx)_s = -[\![\varphi_x]\!]/[\![\varphi_y]\!] \quad (5b)$$

where $[\![(\cdots)]\!]$ and $\overline{(\cdots)}$ indicate the jump in and average of $(\cdots)$ across the shock wave. Equation (5a) insures the conservation of mass. The conservation of momentum is replaced by the irrotationality condition Eq. (5b) or its equivalent, $[\![\phi]\!] = 0$.

Time-linearization

We use the ADI technique introduced by Ballhaus and Steger (12) to compute the steady state solution of Eq. (1), $\varphi_o(x,y)$, subject to the steady boundary conditions implied by Eqs. (1)-(4), using the *coordinate stretching of Ref.* (13). Aside from the far-field condition (4) and the inclusion of terms of O(k) relative to O(1) in (2) and (3), this is equivalent to NASA Ames computer code LTRAN2 of Ballhaus and Goorjian (14). We next linearize about this steady state by assuming that

$$\varphi(x,y,t) = \varphi_o(x,y) + (\tilde{\delta}/\delta_o^{3/2})\tilde{\varphi}(x,y,t) + o(\tilde{\delta}/\delta_o^{3/2}),$$

where $\tilde{\delta}/\delta_o^{3/2} = o(1)$. This gives, with $\delta = \delta_o$,

$$-(2kM_\infty^2/\delta_o)\tilde{\varphi}_{xt} + \{[(1 - M_\infty^2)/\delta_o$$
$$-(\gamma + 1)M_\infty^2\varphi_{ox}]\,\tilde{\varphi}_x\}_x + \tilde{\varphi}_{yy} = 0, \quad (6a)$$

with

$$\tilde{\varphi}_y(x,o,t) = \tilde{Y}_x(x,t) + k\tilde{Y}_t(x,t) \quad (6b)$$

and

$$[\![\tilde{\varphi}_x(x,o,t) + k\tilde{\varphi}_t(x,o,t)]\!] = 0. \quad (6c)$$

With the linearization of the solution about a steady state at time t = 0, we use (4) for the potential far from the airfoil as the circulation departs from its steady state value.

As noted earlier, the proper account shock motions are of prime importance in unsteady transonic flow. We thus use the procedure of Ref. (13) to account for shock motions. Because the shock waves are nearly normal to the freestream we assume that this is the case and satisfy

$$[\![\phi]\!] = 0$$

on the normal shock approximation to Eq. (5), viz.,

$$\frac{dx}{dt}_s = + \frac{\gamma + 1}{2k} \{ \frac{M_\infty^2 - 1}{(\gamma+1)M_\infty^2} + \tilde{\phi}_x \}.$$

Again we linearize about the steady state, writing in this approximation

$$x_s(t) = x_{os} + (\tilde{\delta}/\delta_o^{3/2})\chi(t)$$

which gives

$$\frac{d\chi(t)}{dt} = \frac{\gamma + 1}{2k} \tilde{\phi}_x(x_{os}, o, t) \qquad (7)$$

as the equation that keeps track of the shock wave position. Straightforward linearization of $[\![\phi_o + (\tilde{\delta}/\delta_o^{3/2})\tilde{\phi}]\!] = 0$ gives the expression that determines $\tilde{\phi}$ behind the shock from its value ahead of the shock (13):

$$[\![\tilde{\phi}(x_s, t, y)]\!] =$$

$$- \frac{\gamma + 1}{2k} [\![\phi_{ox}(x_s', y)]\!] \int_o^t \tilde{\phi}(x_s', o, \hat{t}) d\hat{t}. \qquad (8)$$

This must be integrated in conjunction with (6a). The ADI procedure is again adopted as outlined in Ref. (13), to effect a solution of Eq. (6) in conjunction with Eq. (8), subject to the time-linearized boundary conditions at Eqs. (6a) and (6b).

INDICIAL RESPONSE

One of the major advantages of time-linearization is that, for a given mode of motion, the amplitude and phase lag of the lift or moment coefficient for a given reduced frequency may be computed by a linear superposition of the results obtained for a step change. For example, if the change in lift coefficient as a function of time for a step change in angle of attack, C_{ℓ_α}, is that sketched in Fig. 2, then the lift coefficient for an angle of attack variation, $\alpha(t)$, is

$$C_{\ell_\alpha}(t) = C_{\ell_\alpha}(t)\alpha(o) + \int_o^t C_{\ell_\alpha}(\tau) \frac{d\alpha(t-\tau)}{d\tau} d\tau. \qquad (9a)$$

Thus, for a periodic motion $\alpha(t) = \alpha_o + \tilde{\alpha} e^{i\omega t}$,

$$C_\ell(t) = \tilde{\alpha} e^{i\omega t} [C_{\ell_\alpha}(\infty) - i\omega \int_o^\infty [C_{\ell_\alpha}(\infty) - C_{\ell_\alpha}(\tau)] e^{-i\omega\tau} d\tau] \qquad (9b)$$

$$+ C_{\ell_\alpha}(\infty)\alpha_o.$$

The low frequency approximation made in Eq. (1), viz., that $k^2\phi_{tt}$ was negligible, is, of course, not valid for the high-frequency components of the indicial response calculation. It is, however, perfectly satisfactory for the computation of the indicial response, provided this response is only used to compute motions for which $k = o(1)$. In order to calculate the response for low reduced frequencies, however, we must accurately resolve the indicial response as the motion approaches its asymptotic state. Typically, this requires the computation of the indicial response for 300 chord lengths of airfoil motion. In this time the unsteady perturbations have travelled a little more than 300 chord lengths normal to the freestream. As a consequence, any boundary condition imposed on a $|y|$ = constant boundary that is less than 150 chord lengths away can contaminate the indicial response through a reflection from a boundary. Our experience has been that an erroneous boundary condition such as $\phi = 0$ has to be imposed at $|y|$ greater than 80 chord lengths in order to avoid errors in the phase lag determined from an indicial response. The same must be true for the computation of a harmonic motion, although it would be more difficult to determine that the phase lag was in error in such a computation. This same observation should also be applied to unsteady wind tunnel tests. If there are significant acoustic reflections from the wind tunnel walls, the observed phase lags may be in error. This experimental difficulty warrants further investigation, especially in two-dimensional studies.

On the other hand, we know that with the appropriate steady state value of the potential applied at about twenty chord lengths, the steady state solution is perfectly adequate. With the imposition of the unsteady boundary condition (4), or its time-linearized analog, we find that once again 20 chord lengths will suffice. For low to moderate reduced frequencies, viz., $k = 0.1$ to 1.0, the acoustic wavelengths associated with the motion are about 1.0 to 10 chords. The grid spacing employed may be stretched, but grid spacing comparable to or larger than the acoustic wavelength will result in acoustic reflections from the grid itself. Thus, while a grid stretching is employed in the calculations, the largest grid spacing used remains a fraction of a chord length.

Harmonic Oscillator Modeling

Typically, the indicial response of the lift coefficient to a step change in angle of attack, flap angle, or imposition of plunging velocity, is like that as shown in Fig. 2. The same is also approximately true for the moment coefficient taken about the airfoil's leading edge (Fig.3). This suggests that, to a first approximation, the response is nearly exponential and governed by a simple first-order differential equation. And, further, that to a second approximation, the difference between this response and an exponential function can be modeled by a damped harmonic oscillator. Thus, if we let $u(t)$ be a normalized indicial response such that $u(0) = -1$, $u(\infty) = 0$, we should write

$$u(t) = 1 + u_o(t) + u_1(t) + \cdots \qquad (10)$$

where

$$L_o u_o \equiv \dot{u}_o + \lambda u_o = 0$$

and, in general,

$$L_i u_i \equiv \ddot{u}_i + 2p_i \dot{u} + q_i u_i = 0.$$

The constants λ, p_i, q_i are determined to best model the indicial response. That is, the solutions to these equations, viz.,

$$u_o(t) = e^{-\lambda t} \qquad (12a)$$

and

$$u_i(t) = u_i(o) e^{-p_i t} \sin(\Omega t)/\Omega, \qquad (12b)$$

where

$$\Omega = \sqrt{(q_1 - p_1^2)},$$

are combined to best approximate the indicial response. To be specific, if we let $\varepsilon_o = u(t) - u_o(t)$, then we choose λ such that

$$I_o(\lambda) = \int_0^\infty [L_o \varepsilon_o]^2 dt \tag{13}$$

is minimum. Setting $\partial I_o/\partial\lambda = 0$, we find

$$\lambda^{-1} = 2\int_0^\infty \{1 - u(t)\}^2 dt. \tag{14}$$

In an analogous manner we let $\varepsilon_1 = u(t) - 1 - u_o(t) - u_1(t)$ and choose p_1 and q_1 so that

$$I_1(p_1, q_1) = \int_0^\infty [L_1 \varepsilon_1]^2 dt \tag{15}$$

is minimized. This gives

$$p_1 = \frac{(\dot{u}(o) - \lambda)^2}{2\int_0^\infty (\dot{u} - \dot{u}_o)^2 dt} \text{ and } q_1 = \frac{\int_0^\infty (\dot{u} - \dot{u}_o)^2 dt}{\int_0^\infty (u - u_o) dt}. \tag{16}$$

The extent to which the simple first approximation is justified for selected examples is shown in Figs. (4) and (5). In many instances an acceptable determination of the phase lag requires the second approximation. This will be discussed more fully in (7). The constant λ and the $I_o(\lambda)$ of the first approximation can be determined immediately from Eqs. (13) and (14) as the indicial response is being calculated. If I_o is not sufficiently small, then the constants p_1 and q_1 can be calculated from Eqs. (16). If the second approximation is not judged sufficiently accurate because I_1 is not acceptably small, the modeling is abandoned as the computational expense of computing p_1 and q_1 is comparable to that required for three reduced frequencies.

Some time ago it was noted by Tijdeman (15) and the authors (13) that the amplitude of a harmonic response decays like k^{-1} with increasing k. A somewhat more general result is implied by Eqs. (12). If F(t) is a harmonic response, e.g., $C_{l_\alpha}(t)$, then with

$$F(t) = F_o(t) + F_1(t) + \cdots, \tag{17}$$

we find that the first approximation gives

$$F_o/A = (1 + k'^2)^{-\frac{1}{2}} \sin(kt - \theta_o) \tag{18a}$$

where

$$\sin\theta_o = k'/(1 + k'^2)^{1/2}. \tag{18b}$$

Here A is the amplitude of the indicial response to a unit change and $k' = k/\lambda$. The second approximation gives

$$F_1/A = \dot{u}_1(o) k' \Omega' \sin(kt - \theta_1) + [\{1 + (k' + \Omega')^2\}\{1 + (k' - \Omega')^2\}]^{1/2} \tag{19a}$$

where

$$\sin\theta_1 = (k'^2 - \Omega'^2 - 1) \div \{[1 + (k' + \Omega')^2][1 + (k' - \Omega')^2]\}^{1/2} \tag{19b}$$

and $\Omega' = \Omega/\lambda$.

We see immediately from Eq. (18) that in the first approximation the amplitude of the harmonic response is

$$[1 + (k/\lambda)^2]^{-1/2}$$

as indicated in Fig. 4, which behaves like k^{-1} for large k, and that the phase lag is

$$\sin^{-1}\{(k/\lambda)/\{1 + (k/\lambda)^2\}^{1/2}$$

which grows linearly with k/λ for small k/λ, and thereafrer is nearly independent of k/λ, as can be seen from Fig. (5).

We limit our discussion to the simple variation of the amplitude and phase lag of the lift and moment coefficients for an NACA 64A006 in pitch with reduced frequency. Earlier, more detailed results depicting the shock motion, etc., are to be found in Refs. (13) and (16). Because we have linearized about a steady, small perturbation solution, we draw no practical conclusions from our study. Tijdeman (personal communication) reports that the application of LTRAN2 to determine the response about an experimental steady state for the F29 airfoil at varying incidence, in conjunction with strip theory and the results of panel methods for subcritical flow to account for three-dimensional effects, was successful in predicting the flutter boundary of the F29 wing.

Figures 4 and 5 give the amplitudes and phase lags of the lift and moment coefficients for an NACA 64A006 airfoil oscillating in pitch at selected reduced frequencies with $M_\infty = 0.86$ and 0.88. Individual results are shown by symbols with the reduced frequency noted below them. Generally, they are well described by the first approximation of the harmonic oscillater model. For $M_\infty = 0.86$ the lift and mid-chord moment results are indistinquishable, but their phase lags are not correctly captured by the modeling of the first approximation. In this case, the initial part of the indicial response is not correctly captured. This is easily dealt with in the model without going to the second approximation (7).

COMPUTATIONAL EFFORT

As noted earlier, a time-linearized calculation requires substantially less computational effort than a nonlinear one. We delineate those differences here, noting that the larger grid spacing that may be used with our shock-fitting procedure implies a computational saving in addition to the considerations discussed here.

If we let T represent the number of time steps required to calculate a time periodic solution in an L×M×N spacial domain, then the total computational effort for a flutter study using either a nonlinear or time-linearized algorithm is proportional to the product TLMN. If we do not time-linearize, this must be done at K reduced frequencies to give a total computational effort that is proportional to KTLMN. If a time-linearized procedure is used to compute a single indicial

response, the effort is TLMN. This can be used to generate the mode response for any reduced frequency in about T^2 additional steps, giving a total computational effort proportional to TLMN + (const)$\cdot T^2K$. Typically, T is 500 and L,M,N are about 50, 25, 25, respectively. Thus, a nonlinear analysis at ten reduced frequencies has a computational effort of about

$$10 \cdot 500 \cdot 50 \cdot 25 \cdot 25 = 10^8.$$

On the other hand, a time-linearized computation requires a computational effort of

$$500 \cdot 50 \cdot 25 \cdot 25 +$$

$$(\text{const})\ (500)^2 10 = 10^7 + (\text{const}) \cdot 10^6$$

providing a factor of K reduction over the nonlinear analysis. The constant of proportionality, and the less refined L grid spacing required, also favor the time-linearized algorithm, contributing roughly another factor of ten reduction over the nonlinear procedure.

In two dimensions, the two computational components of the time-linearized calculation, viz., the indicial response and its linear superposition for each reduced frequency, are comparable and an efficient integration algorithm must be used for Eq. (9b).

CONCLUSION

The amplitudes and phase lags of the lift and moment coefficients, at selected reduced frequencies, can be computed accurately and efficiently by time-linearization about a measured or computed pressure field. For three-dimensional studies the linear superposition of the results of a single indicial response substantially reduces the computational effort. Further reductions are achieved by using the linearized far-field for the unsteady flow, and by treating the shock wave as a discontinuity in the computations. In many cases, the indicial response can be modeled by a simple harmonic oscillator, and this provides an analytical result for the dependence of the lift and moment coefficients on reduced frequency, further reducing the computational effort.

ACKNOWLEDGMENTS

This research was supported by ONR Contract Number N00014-76-C-0182 and by AFOSR Grant Number AFOSR-76-2954I. The authors are greatly indebted to Mr. Morton Cooper for his support of their efforts to develop a program in analytical and computational aerodynamics at the University of Arizona.

REFERENCES

1. Farmer, M. G. and Hanson, P. W., "Comparison of Supercritical and Conventional Wing Flutter Characteristics," Proceedings AIAA/ASME/SAE 17th Structures, Structural Dynamics and Materials Conf., King of Prussia, Pa., April 1976, pp. 608-611.

2. Tijdeman, H. and Seebass, R., "Transonic Flow Past Oscillating Airfoils," Ann. Rev. Fluid Mech. 1980, 12, pp. 181-222.

3. Traci, R. M., Farr, J. L., and Albano, E., "Perturbation Method for Transonic Flows About Oscillating Airfoils," AIAA Paper 75-877, 1977.

4. Weatherill, W. H., Sebastian, J. D., and Ehlers, F. E., "Application of a Finite Difference Method to the Analysis of Transonic Flow Over Oscillating Airfoils and Wings," AGARD-CP-226, 1977.

5. Weatherill, W. H., Sebastian, J. D., and Ehlers, F. E., "The Practical Application of a Finite Difference Method of Analyzing Transonic Flow Over Oscillating Airfoils and Wings," NASA Contract Rep. 2933, 1978.

6. Fung, K-Y., "Far-Field Boundary Conditions for Unsteady Transonic Flows," (to appear AIAA J.).

7. Fung, K-Y., "A Time-Linearized Algorithm for Unsteady Transonic Flow," (in preparation).

8. Melnik, R. E., "Turbulent Interactions on Airfoils at Transonic Speeds-Recent Developments," AGARD Symposium on Computation of Viscous-Inviscid Flows, Cororado Springs, October 1980.

9. Lin, C. C., Reissner, E., and Tsien, H. S., "On Two-Dimensional Non-Steady Motion of a Slender Body in a Compressible Fluid," J. Math. Phys. 3, pp. 220-31, 1948.

10. Couston, M. and Angelini, J. J., "Solution of Nonsteady Two-Dimensional Transonic Small Disturbances Potential Flow Equation," In Nonsteady Fluid Dynamics: Proc. ASME Winter Annual Mtg., Dec. 10-15, 1978, San Francisco, pp. 233-44. See also ONERA TP-No. 1978-69.

11. Houwink, R. and van der Vooren, J., "Results of an Improved Version of LTRAN-2 for Computing Unsteady Airloads on Airfoils Oscillating in Transonic Flow," AIAA Paper 79-1553, 1979.

12. Ballhaus, W. F. and Steger, J. L., "Implicit Approximate-factorization Schemes for the Low-frequency Transonic Equation," NASA Tech. Memo TM X-73,082, 1975.

13. Fung, K-Y., Yu, N. J. and Seebass, R., "Small Unsteady Perturbations in Transonic Flows," AIAA J., 16, pp. 815-22, 1978.

14. Ballhaus, W. F. and Goorjian, P. M., "Implicit Finite-difference Computations of Unsteady Transonic Flows About Airfoils," AIAA J., 15, 1728-35, 1977.

15. Tijdeman, H., "Investigations of the Transonic Flow Around Oscillating Airfoils," Doctoral Thesis. Technische Hogeschool, Delft, The Netherlands, 148 pp., 1977.

16. Seebass, A. R., Yu, N. J. and Fung, K-Y., "Unsteady Transonic Flow Computations," AGARD-CP-227, 1978.

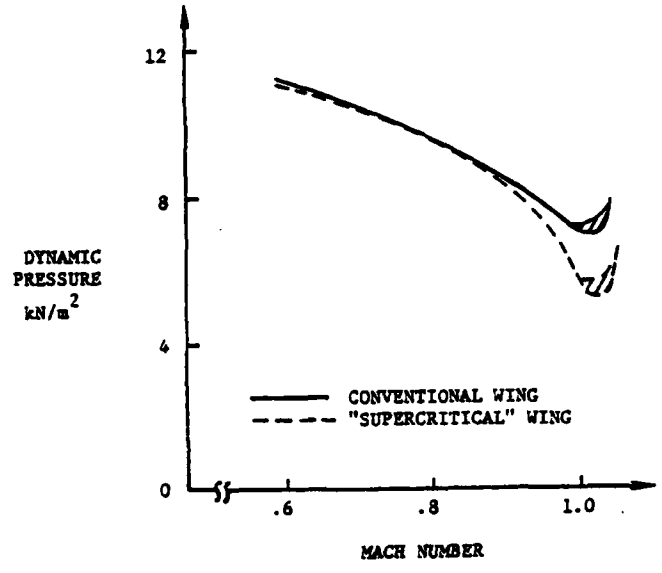

Figure 1. Flutter boundary for two dynamically identical TF-8A wings (Reference (1)).

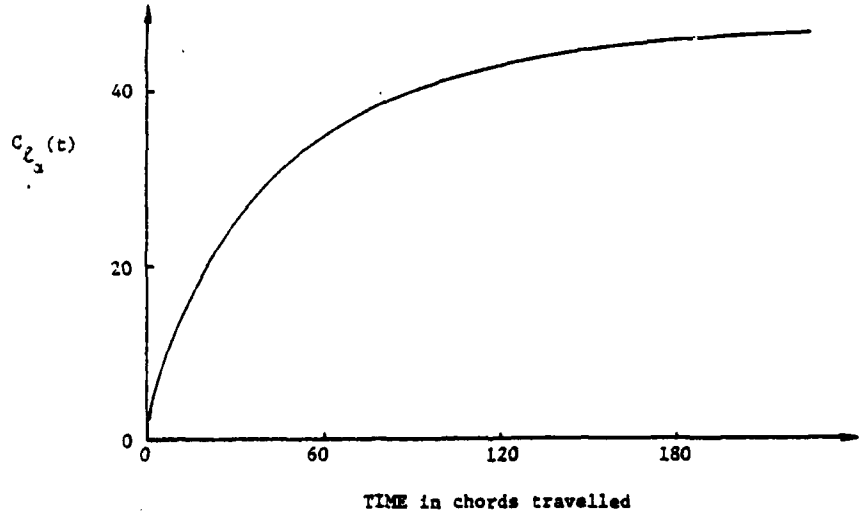

Figure 2. Lift coefficient as a function of time for a step change in angle of attack; NACA 64A006, $M_\infty = 0.88$.

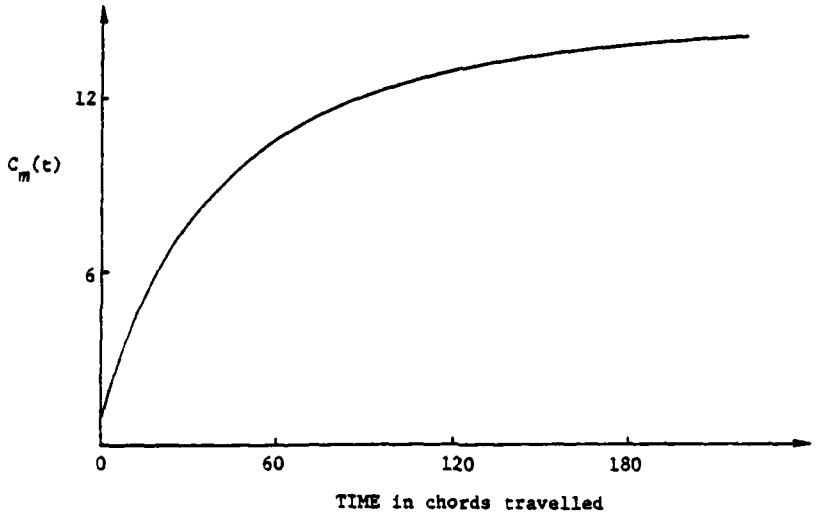

Figure 3. Moment coefficient as a function of time for a step change in angle of attack; NACA 64A006, $M_\infty = 0.88$.

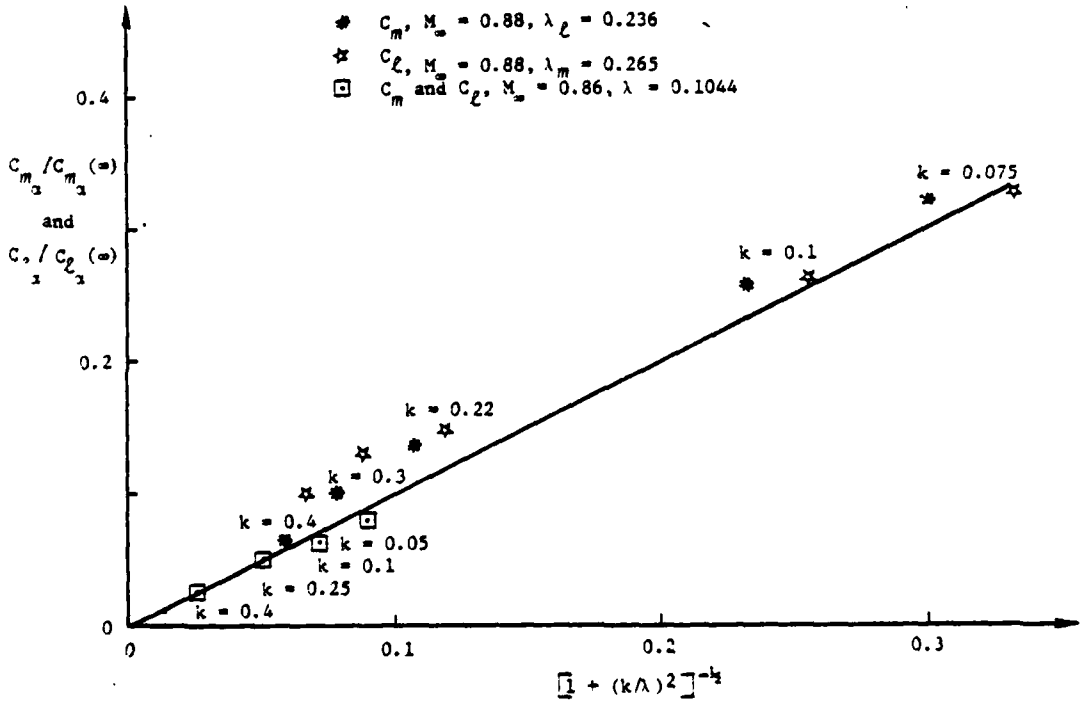

Figure 4. Lift and moment amplitudes normalized by their quasi-steady value as a function reduced frequency for an NACA 64A006 airfoil.

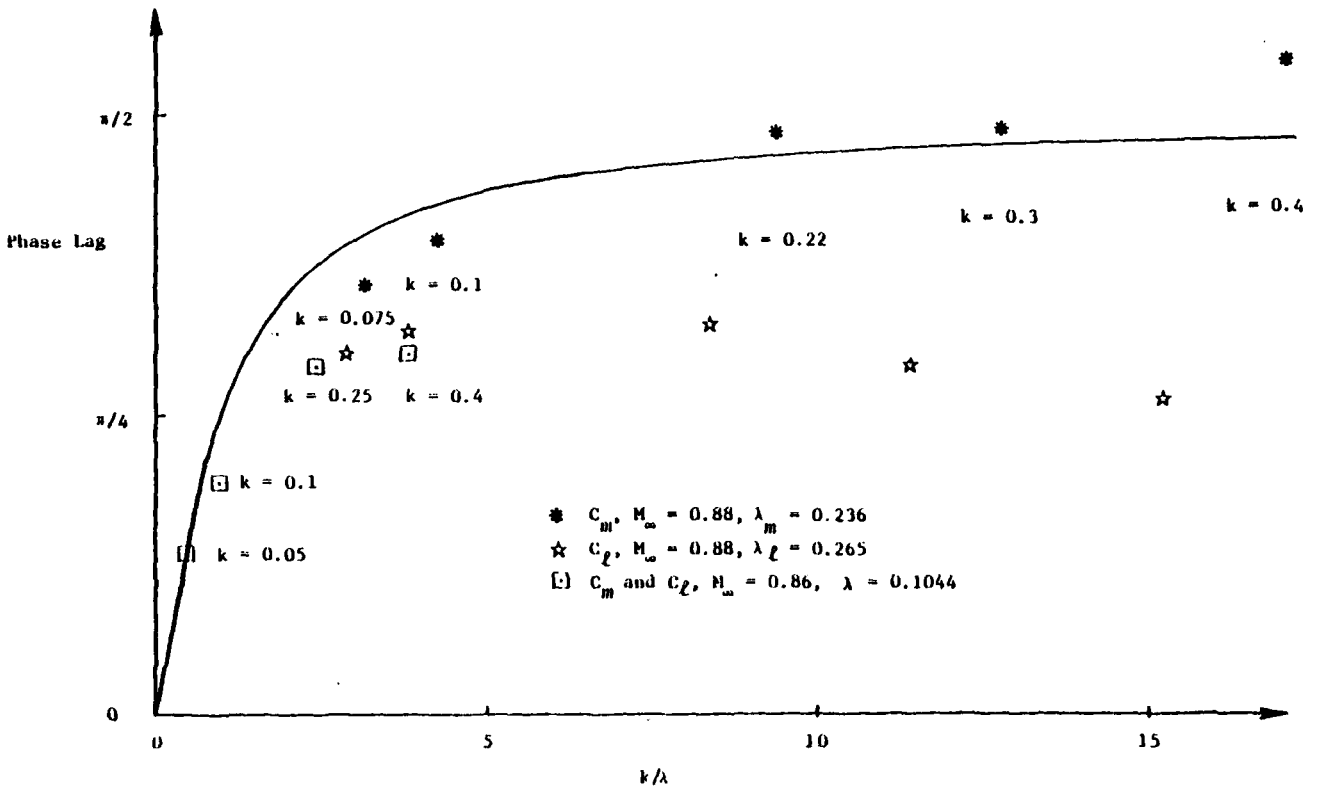

Figure 5. Phase lag for the lift and moment as a function of reduced frequency for an NACA 64A006 airfoil.


F
8